ENVIRONMENTAL RESEARCH
LETTERS

LETTER • OPEN ACCESS

Tipping point in North American Arctic-Boreal carbon sink persists in new generation Earth system models despite reduced uncertainty

To cite this article: Renato K Braghiere *et al* 2023 *Environ. Res. Lett.* **18** 025008

ENVIRONMENTAL RESEARCH
LETTERS

LETTER

Tipping point in North American Arctic-Boreal carbon sink persists in new generation Earth system models despite reduced uncertainty

Renato K Braghiere[1,2,*], **Joshua B Fisher**[3], **Kimberley R Miner**[2], **Charles E Miller**[2], **John R Worden**[2], **David S Schimel**[2] and **Christian Frankenberg**[1,2]

[1] Division of Geological and Planetary Sciences, California Institute of Technology, Pasadena, CA 91125, United States of America
[2] Jet Propulsion Laboratory, California Institute of Technology, 4800 Oak Grove Drive, Pasadena, CA 91109, United States of America
[3] Schmid College of Science and Technology, Chapman University, Orange, CA 92866, United States of America
[*] Author to whom any correspondence should be addressed.

E-mail: renato.k.braghiere@jpl.nasa.gov

Keywords: NASA ABoVE, CMIP5, CMIP6, tipping point, carbon cycle, soil carbon

Supplementary material for this article is available online

OPEN ACCESS

RECEIVED
19 May 2022

REVISED
20 December 2022

ACCEPTED FOR PUBLICATION
11 January 2023

PUBLISHED
10 February 2023

Abstract

Estimating the impacts of climate change on the global carbon cycle relies on projections from Earth system models (ESMs). While ESMs currently project large warming in the high northern latitudes, the magnitude and sign of the future carbon balance of Arctic-Boreal ecosystems are highly uncertain. The new generation of increased complexity ESMs in the Intergovernmental Panel on Climate Change Sixth Assessment Report (IPCC AR6) is intended to improve future climate projections. Here, we benchmark the Coupled Model Intercomparison Project (CMIP) 5 and 6 (8 CMIP5 members and 12 CMIP6 members) with the International Land Model Benchmarking (ILAMB) tool over the region of NASA's Arctic-Boreal vulnerability experiment (ABoVE) in North America. We show that the projected average net biome production (NBP) in 2100 from CMIP6 is higher than that from CMIP5 in the ABoVE domain, despite the model spread being slightly narrower. Overall, CMIP6 shows better agreement with contemporary observed carbon cycle variables (photosynthesis, respiration, biomass) than CMIP5, except for soil carbon and turnover time. Although both CMIP ensemble members project the ABoVE domain will remain a carbon sink by the end of the 21st century, the sink strength in CMIP6 increases with CO_2 emissions. CMIP5 and CMIP6 ensembles indicate a tipping point defined here as a negative inflection point in the NBP curve by 2050–2080 independently of the shared socioeconomic pathway (SSP) for CMIP6 or representative concentration pathway (RCP) for CMIP5. The model ensembles therefore suggest that, if the carbon sink strength keeps declining throughout the 21st century, the Arctic-Boreal ecosystems in North America may become a carbon source over the next century.

1. Introduction

Global mean surface temperatures have increased dramatically since the mid-20th century, but have increased up to four times faster in the Arctic-Boreal region (Masson-Delmotte *et al* 2021, Rantanen *et al* 2022). This phenomenon is referred to as 'arctic amplification' (Scheffer *et al* 2012, Francis *et al* 2017). Although the exact mechanisms for the arctic amplification are debated, temperature and snow-sea ice-albedo feedbacks are keys to understanding this system, and changes in atmospheric and ocean energy transport may play an important role (Previdi *et al* 2021). While Arctic-Boreal ecosystem productivity may initially benefit from rising atmospheric CO_2, higher temperatures, longer growing seasons, and faster nutrient cycling, these same systems may increase carbon emissions through permafrost thaw, plant (autotrophic) respiration and increased microbial (heterotrophic) respiration (Mack *et al* 2004,

Natali *et al* 2012, 2019, Crowther *et al* 2015, Schuur *et al* 2015, Koven *et al* 2017, Huntzinger *et al* 2020, Miner *et al* 2022).

Projecting the future trajectory of the Arctic-Boreal system presents a large challenge to Earth system models (ESMs) (Hinzman *et al* 2013) and requires critical cryosphere-specific processes to accurately model its physical, biogeochemical and ecosystem dynamics (including carbon) (Hawkins and Sutton 2009, Knutti and Sedláček 2013, Slater and Lawrence 2013, Koven *et al* 2015, Lawrence *et al* 2015, Schimel *et al* 2015, Ciais *et al* 2019, Braghiere *et al* 2021b, 2022). The Coupled Model Intercomparison Project Phase 6 (CMIP6; Eyring *et al* 2016) is the most recent ESM activity, and builds upon CMIP5 (Taylor *et al* 2012), interpreted in the IPCC Fifth Assessment Report (Intergovernmental Panel on Climate Change 2014). CMIP6 includes the latest generation of comprehensive ESMs, driven by historical greenhouse gas concentrations and climate forcing followed by different future greenhouse gas concentrations pathways according to the shared socioeconomic pathways (SSPs) scenarios (Meinshausen *et al* 2020, Tokarska *et al* 2020). The SSPs picture multiple baseline worlds considering underlying factors, such as population, technological, and economic growth, and how those could lead to different future scenarios and global change outcomes. That does not imply a larger uncertainty in climate change, it rather considers different economic and political choices.

While benchmarking and validation of ESMs has become increasingly common in recent years (Fisher JB *et al* 2018), it is still rare to comparatively evaluate the performance of a carbon cycle model once it is updated (Fer *et al* 2021). However, comparing models and observations is required for hypothesis testing and predictive skill evaluation (Fisher RA *et al* 2018). To this end, the International Land Model Benchmarking (ILAMB) project (Hoffman *et al* 2017, Collier *et al* 2018) provides the means to track and compare performance through a comprehensive skill score method and to incorporate multiple observational datasets of the same variable of interest to account for observational uncertainty. Moreover, greater agreement between historical runs and observations may indicate that model components can be updated to better capture inaccurate processes. This would increase confidence in future projections, even though forthcoming changes, such as photosynthesis acclimation or species composition shifts, may become progressively more important.

Whether Arctic-Boreal ecosystems will evolve into significant carbon sinks (Keenan *et al* 2014, Zhu *et al* 2016, Berner *et al* 2020), net carbon sources (Hayes *et al* 2011, Zhang *et al* 2022), or remain nearly carbon neutral (McGuire *et al* 2012) depends on the trajectory of climate change (McGuire *et al* 2018, de Vrese and Brovkin 2021, De Vrese *et al* 2021). It is also imperative to understand if ESMs accurately describe the major carbon cycle fluxes, storage terms, and processes in the present. The critical threshold at which a perturbation can qualitatively alter the system's state or development is referred to as a tipping point (Lenton *et al* 2008). An Arctic-Boreal carbon cycle tipping point would occur when the rate of release of previously frozen soil carbon to the atmosphere by ecosystem respiration and disturbances (DISTs), including wildfires, surpasses photosynthetic CO_2 uptake (Ahlström *et al* 2015). This permafrost carbon feedback (Schuur *et al* 2015, Miner *et al* 2022) has been identified as a critical Earth system tipping point (Lenton *et al* 2008, McKay *et al* 2022). For example, the rapid warming of the Arctic-Boreal zone has accelerated permafrost degradation (Mekonnen *et al* 2021) and is remaking the vast, conifer-dominated boreal forests, lowering species diversity, increasing ecosystem vulnerability to disease, decreasing vegetation reproduction rates, making fires more frequent and intense, and increasing mortality rates (Lenton 2012, Seidl *et al* 2017). In a stark example of this from the mid-1990s, summer warming in the absence of sustained increases in precipitation breached the tipping point in western central Eurasian boreal forests, sharply shifting ecosystems into a warmer and drier regime (Buermann *et al* 2014). Ensuring that ESMs reproduce emergent Arctic-Boreal ecosystem tipping points requires considerable certainty in both ecosystem stability and carbon cycle drivers. Unfortunately, both of these complex, interconnected systems are largely unconstrained within ESMs.

The goal to reduce carbon cycle uncertainty is non-trivial (Hausfather *et al* 2022) and it can be bounded by inherent model uncertainties encompassing parametric and structural uncertainty, as well as forcing data uncertainty (Lovenduski and Bonan 2017). Yet, interpreting model spread as predictive failure would not bring as much benefit to science as much as a comprehensive discussion of model uncertainty (Bonan *et al* 2019). To this end, we compare projections of the carbon cycle variables from CMIP5 and CMIP6 over Alaska and northwestern Canada, the domain of NASA's Arctic-Boreal vulnerability experiment (ABoVE; figure S1). We benchmark the historical runs with a suite of state-of-the-art Earth observations to test if the most recent models converge in their projections of the Arctic-Boreal carbon cycle.

The rationale behind benchmarking models in the historical period before evaluating their future projections is related to the hypothesis that a model (or group of models) that better represents the present has greater predictive skills, and therefore, should better represent the future. Although mechanistic processes represented in these models could potentially change in the future (i.e. acclimate), the

predictive skill of two model groups can only be evaluated with historical datasets. We compare model performances and uncertainty, identify improvements and deterioration from older ESMs to newer ones, and analyze modeled carbon uptake growing curves to determine if these models project a potential Arctic-Boreal carbon balance tipping point.

2. Material and methods

2.1. Study domain and models

This study focuses on the ABoVE domain, including the Arctic and Boreal regions of Alaska, and the western provinces of Canada (Fisher JB *et al* 2018, Stofferahn *et al* 2019, Huntzinger *et al* 2020). We benchmark six ecosystem and carbon cycle variables: above-ground biomass, gross primary productivity (GPP), ecosystem respiration (RECO), leaf area index (LAI), net ecosystem exchange (NEE), and topsoil carbon. We incorporate 3 meteorological forcing datasets (i.e. surface air temperature, precipitation, and surface downward shortwave radiation), output from a total of 20 CMIP models, with 8 models participating in the CMIP5 and the remaining 12 latest model versions participating in the CMIP6 (table 1). These models were chosen based on the availability of all the required variables included in the analysis. We also evaluated monthly historical simulations (1850–2005 for CMIP5 and 1850–2015 for CMIP6) driven by observation-based forcing data, including greenhouse gas concentrations, gridded land-use data, volcanic aerosols, and other meteorological variables (Eyring *et al* 2016).

Previously, in preparation for CMIP5, the land-use harmonization v1 (LUH1) project provided harmonized land use data for the years 1500–2100 at 0.5 deg × 0.5 deg resolution (Hurtt *et al* 2011). These data served as required land use forcing for CMIP5 climate model experiments and have been used in a number of related studies to assess the effects of land use change on carbon cycle and climate. More recently, as part of CMIP6 (Eyring *et al* 2016), the international research community has developed the next generation of advanced ESMs able to estimate the combined effects of human activities (e.g. land use and fossil fuel emissions) on the carbon–climate system. The strategy described in the updated LUH2 builds on the approach for harmonizing land use patterns and transitions in CMIP5. The new version is completely updated with new inputs and includes higher spatial resolution (0.25 deg vs. 0.5 deg), increased detail (12 states vs. 5 and all associated transitions), added management layers, new future scenarios (8 vs. 4), and a longer time domain (850–2100 vs. 1500–2100)—in all more than a 50-fold increase in data from its predecessor (Hurtt *et al* 2020). Despite these differences, carbon fluxes associated with DISTs are several orders of magnitude smaller than photosynthesis and respiratory terms (see figure S2 in supporting information).

CMIP models provide multiple simulations based on the different experimental configurations for ensemble member analyses to capture the climate system's natural variability. However, some of the participant members have only released their first realization, denominated as r1i1f1; therefore, we utilized the first realization only, following previous recommendations (Anav *et al* 2013, Park and Jeong 2021).

2.2. Model benchmarking

We used the ILAMB v2.6 package for model benchmarking (Collier *et al* 2018) focusing on global patterns of ecosystem and carbon cycle variables, including datasets: (a) aboveground living biomass based on inventory plots upscaled using remote sensing imagery from GlobalCarbon (Saatchi *et al* 2011), USForest (Blackard *et al* 2008), and Thurner (Thurner *et al* 2014); (b) GPP and RECO from FLUXCOM (Jung *et al* 2019, 2020) and from FLUXNET2015 (Pastorello *et al* 2020); (c) LAI from the moderate resolution imaging spectroradiometer (MODIS) (De Kauwe *et al* 2011), AVHRR and AVH15C1 (Claverie *et al* 2016); (d) NEE from global bio-atmosphere flux (GBAF) (Jung *et al* 2010) and FLUXNET2015 (Pastorello *et al* 2020); and (e) soil carbon stocks from the Harmonized World Soil v1.2 Database (HWSD; Nachtergaele *et al* 2012), the Northern Circumpolar Soil Carbon Database version 2.2 (NCSCDv2.2) (Hugelius *et al* 2013a, 2013b), and soil carbon turnover time (Koven *et al* 2017). Results from the global models were masked out to focus benchmarking on the ABoVE domain.

The relationships between these variables and precipitation, temperature, and incident shortwave radiation were analyzed using data products from the Global Precipitation Climatology Project Monthly Analysis version (Adler *et al* 2018), the Climatic Research Unit monthly temperature version 4.02 (Harris *et al* 2014), and the Clouds and the Earth's Radiant Energy System surface irradiances edition 4.1 (Kato *et al* 2018, Loeb *et al* 2018).

We use the results for the ILAMB overall score for the absolute values (S_{overall}) defined as:

$$S_{\text{overall}} = \frac{S_{\text{bias}} + 2S_{\text{RMSE}} + S_{\text{phase}} + S_{\text{dist}}}{1+2+1+1} \qquad (1.1)$$

where S_{bias} is the spatially integrated bias score, S_{RMSE} is the root-mean-squared error (RMSE) score doubly weighted to emphasize its importance, S_{phase} is the phase shift score, and S_{dist} is the spatial distribution score. For the whole set of equations of each term in equation (1) refer to Collier *et al* (2018). All the ILAMB results and plots are available in https://braghiere.github.com (accessed on: April 05th 2022).

Table 1. General specifications of ESMs used in this study.

CMIP5												
Modeling group	ESM	Land model	Number of live carbon pools	Number of dead carbon pools	No of plant functional types (PFTs)	Fire	Dynamic vegetation cover	Nitrogen cycle	Phosphorus cycle	No soil layers	Soil depth (m)	References
CSIRO	ACCESS1-3	CABLE1.8	3	6	13	No	No	Yes	Yes	4	2.0	Kowalczyk *et al* (2013)
CCCMA	CanESM2	CLASS2.7-CTEM	3	2	9	No	No	No	No	3	2.2	Arora and Boer (2005); Arora *et al* (2011)
GFDL	GFDL-ESM2M	LM3	6	4	5	Yes	Yes	No	No	20	8.8	Shevliakova *et al* (2009); Shao *et al* (2013)
UK	HadGEM2-CC	JULES	3	4	5	No	Yes	Yes	No	4	2.0	(Martin *et al* 2011, Best *et al* 2011, Clark *et al* 2011)
IPSL	IPSL-CM5A-LR	ORCHIDEE	8	3	15	No	No	No	No	7	3.9	(Dufresne *et al* 2013, Krinner *et al* 2005)
JAMSTEC	MIROC-ESM	MATSIRO (physics) VISIT-e (BGC)	3	6	13	No	No	Yes	No	6	9.0	(Watanabe *et al* 2011, Sato *et al* 2007)
MPI	MPI-ESM-LR	JSBACH	3	18	13	Yes	Yes	Yes	No	5	7.0	(Giorgetta *et al* 2013, Raddatz *et al* 2007, Knorr 2000)
NCC	NorESM1-M	CLM4	22	7	22	Yes	No	Yes	No	15	35.2	(Iversen *et al* 2013, Bentsen *et al* 2013)

CMIP6												
Modeling group	ESM	Land model	Number of live carbon pools	Number of dead carbon pools	Number of plant functional types (PFTs)	Fire	Dynamic vegetation cover	Nitrogen cycle	Phosphorus cycle	No. soil layers	Soil depth (m)	Reference
CSIRO	ACCESS-ESM1-5	CABLE2.4 with CASA-CNP	3	6	13	No	No	Yes	Yes	6	2.9	(Bi *et al* 2020)
BCC	BCC-CSM2-MR	BCC-AVIM2	8	16	16	No	No	No	No	10	2.9	(Wu *et al* 2019, Li *et al* 2019)
CCCMA	CanESM5	CLASS3.6-CTEM	3	2	9	No	No	No	No	3	4.1	(Swart *et al* 2019, Arora *et al* 2020)
CESM	CESM2	CLM5	22	7	22	Yes	No	Yes	No	25	42.0	(Danabasoglu *et al* 2020, Lawrence *et al* 2019)
CNRM	CNRM-ESM2-1	ISBA-CTRIP	6	7	16	Yes	No	No (implicit, derived from Yin, 2002)	No	14	10.0	(Delire *et al* 2020)
GFDL	GFDL-ESM4	LM4.1	6	4	5	Yes	Yes	No	No	20	8.8	(Dunne *et al* 2020, Zhao *et al* 2018)
NASA	GISS-E2-1-G	Ent TBM	5	2	17	Yes	Yes	Yes	No	6	2.7	(Ito *et al* 2020)
IPSL	IPSL-CM6A-LR	ORCHIDEE, branch 2.0	8	3	15	No	No	No	No	18	65.6	(Boucher *et al* 2020)
JAMSTEC	MIROC-ESM1-2-LR	MATSIRO (physics) VISIT-e (BGC)	3	6	13	No	No	Yes	No	6	9.0	(Ito and Oikawa 2002)
MPI	MPI-ESM1-2-LR	JSBACH3.2	3	18	13	Yes	Yes	Yes	No	5	7.0	(Mauritsen *et al* 2019)
NCC	NorESM2-LM	CLM5	22	7	22	Yes	No	Yes	No	25	42.0	(Seland *et al* 2020)
UK	UKESM1-0-LL	JULES-ES-1.0	3	4	13	No	Yes	Yes	No	4	2.0	(Sellar *et al* 2019, Walters *et al* 2019)

3. Results

3.1. Benchmarking CMIP models

Modeling if an Arctic-Boreal carbon cycle tipping point will occur is rather complex and dependent on a number of feedback loop interactions, but results indicate newer ESMs are generally better at capturing the present-day carbon cycle picture over the Arctic-Boreal ecosystems than were previous model versions. The exception to the general improvement in more recent ESMs is related to the representation of carbon in soils.

Figure 1 shows the overall scores for ecosystem and carbon cycle variables for the CMIP5 and CMIP6 ensemble members. Results for individual models can be found in supporting information (figure S3). The ensemble member is per definition fluxes and states averaged across individual model members within a modeling group. These use multiple datasets included in the ILAMBv2.6. Triangles corresponding to different ensemble members (CMIP5 and CMIP6) and spatial domains (ABoVE and global) are represented by a schematic in blue. Comparisons between CMIPs globally versus the ABoVE domain is performed to determine if the expected improvements in newer model versions are comparable when only considering the Arctic-Boreal North America.

For aboveground biomass, the CMIP6 ensemble member presents a higher overall score than the CMIP5 ensemble member across all the evaluated data products for the ABoVE domain and the globe. However, the overall score for the ABoVE domain is always smaller than the global overall score for both ensemble members. This suggests that most process-based models included in this study better capture carbon allocation to living stock for other ecosystems and regions of the globe on average than to the Arctic-Boreal North America. The highest overall score between models and biomass datasets is given for Thurner, followed by GlobalCarbon, and USForest.

For GPP and RECO, the CMIP6 ensemble member also presents a higher overall score than the CMIP5 ensemble member across all the evaluated data products for the ABoVE domain and the globe, with the overall score for the ABoVE domain being higher than the global overall score for both ensemble members. The higher score is mainly due to larger bias and RMSE in more productive areas of the globe, including the tropics and temperate forests. For GPP, the overall score related to the FLUXCOM data product is systematically larger than the those associated with FLUXNET2015, while for RECO, CMIP6 over ABoVE presents better agreement for FLUXNET2015 than to FLUXCOM.

Spatiotemporal GPP biases between CMIP5 and CMIP6 with FLUXCOM for the period from 1980 to 2014 are shown in supporting information (figure S4). The positive bias in GPP presented in CMIP5 in the northeastern and east of the ABoVE domain is not observed in CMIP6, as well as a negative bias in GPP in the pacific. A slight ($\sim$1 g $m^{-2}d^{-1}$) positive bias in CMIP6 GPP remains in central parts of the ABoVE domain, as well as southern croplands in Canada. For GPP annual cycle, CMIP6 also presents higher agreement with FLUXCOM (bias = 0.56 g m^{-2} d^{-1}, RMSE = 0.84 g m^{-2} d^{-1}) than CMIP5 (bias = 0.79 g m^{-2} d^{-1}, RMSE = 1.23 g m^{-2} d^{-1}), approximately 30% reduction in bias and RMSE, with especially accurate performance during spring.

To assess the representation of mechanistic processes in the models, we also evaluate variable-to-variable relationships of GPP with precipitation, surface downward shortwave radiation, and temperature. The response curves are then scored by computing a relative error based on the RMSE of reference datasets to the relationship diagnosed in models. Across all the evaluated relationships of GPP with meteorological variables, the scores of CMIP6 were higher than those of CMIP5 (refer to supporting information; figure S5).

For LAI, the CMIP6 ensemble members present a larger overall score than the CMIP5 ensemble members across both spatial domains and data products. Still, the CMIP6 ensemble member over the ABoVE domain presents a larger overall score than the CMIP6 ensemble member over the globe, which is not observed in comparison with AVHRR and AVH15C1.

Spatiotemporal LAI biases between CMIP5 and CMIP6 with MODIS for the period from 2000 to 2006 are shown in supporting information (figure S6). A strong positive bias (>2 m^2 m^{-2}) in LAI presented in CMIP5 in most of the ABoVE domain including Alaska, the northeastern and eastern parts of the domain, as well as the boreal cordillera (higher elevation terrain of the Rocky Mountains and the Coast Mountains) are corrected in CMIP6, as well as a negative bias in LAI in the Pacific coast, boreal plain and taiga plain. A positive bias in CMIP6 LAI remains in high elevation areas, as well as southern croplands in Canada. For LAI annual cycle, CMIP6 also presents higher agreement with MODIS (bias = 0.22 m^2 m^{-2}, RMSE = 0.53 m^2 m^{-2}) than CMIP5 (bias = 0.67 m^2 m^{-2}, RMSE = 0.91 m^2 m^{-2}), approximately 40% reduction in bias and 70% reduction in RMSE, with high performance in the first half of the year and slight overestimation in the second half of the year. Across all the evaluated relationships of LAI with meteorological variables, the scores of CMIP6 were higher than those of CMIP5 (refer to supporting information; figure S7).

Finally, soil carbon overall scores highlight a downgrade in model performance from CMIP5 to CMIP6 for both spatial domains in comparison to the HWSD data product and inferred turnover rates from Koven *et al* (2017) over the globe. In comparison to NCSDV22 soil carbon data, CMIP6 presents a larger overall score than CMIP5 models for both spatial

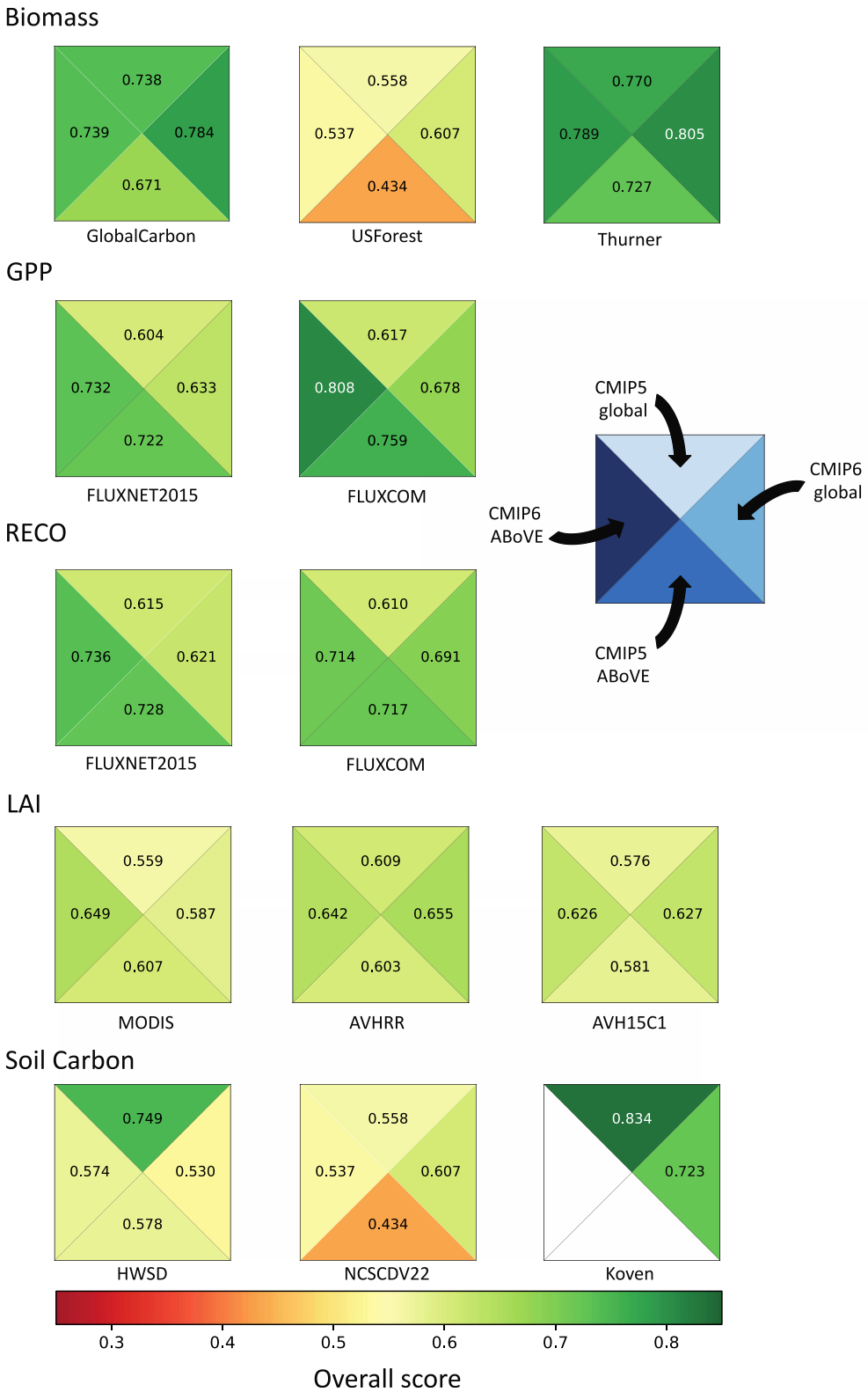

Figure 1. ILAMB2.6 overall scores for ecosystem and carbon cycle variables using multiple datasets. Triangles correspond to different ensemble members (CMIP5 or CMIP6) for different spatial domains (ABoVE or global). Areas in white represent missing data.

domains, but with significantly smaller overall scores over the ABoVE domain (at least 10%). This may suggest that despite the uncertainty associated with empirical datasets, inconclusive discrepancies remain in the consistency of soil carbon estimates with the observations between the two evaluated ESM generations. Significant feedback loops between soil carbon and environmental factors associated with a lack

of improvement in soil carbon representation within updated ESMs may reduce our confidence in future projections of climate change.

In general, CMIP6 overall scores are larger than CMIP5 overall scores for the globe and the ABoVE domain except for one intercompared soil carbon product and turnover rate. It is rather difficult to represent soils within ESMs because they depend on multiple factors such as topography, parent material, environmental factors, and microbial communities, as well as other living beings. Divergence in ESMs arise from incomplete parametric and structural understanding of soil carbon decomposition, as well as uncertainties in model inputs and boundaries, such as climate and plant functional types. An analogous figure to figure 1 showing the climatic forcing metrics is shown in supporting information (figure S8).

3.2. The carbon cycle in the ABoVE domain

Attempts to characterize the global carbon cycle through analyzing the carbon budget lies in understanding fundamental differences between the largest atmosphere-biosphere carbon fluxes, i.e. GPP, net primary productivity (NPP), NEE, and net biome production (NBP). Although highly uncertain (Anav *et al* 2015, Braghiere *et al* 2019, Jian *et al* 2022), the global carbon cycle has been previously estimated with: (a) global GPP being about 120 PgC yr^{-1}, with almost half being lost to autotrophic respiration, resulting in (b) NPP of about 60 PgC yr^{-1}; (c) NEE being the difference between the rate of production of living organic matter (NPP) and the decomposition rate of dead organic matter (heterotrophic respiration), with a negative flux indicating net land carbon uptake. Heterotrophic respiration includes all losses by animals and microbial carbon decomposition by microbes. Global NEE is estimated to be about 10 PgC yr^{-1}, with (d) NBP being the net production of organic matter in a region containing a range of ecosystems and including, in addition to heterotrophic respiration, other processes leading to loss of living and dead organic matter (DISTs such as harvest, forest clearance, fires, insect outbreaks, among others), with a positive flux indicating net land carbon uptake. Global NBP has been considered to be close to zero throughout most of the historical period, but it has been persistently increasing mainly due to the CO_2 fertilization effect and is assumed to be in the order of 1% of NPP and about 10% of NEE (Steffen *et al* 1998, IPCC 2007).

As previously estimated for the whole globe, we use the CMIP5 and CMIP6 ensemble members for the historical period (Hist., 1986–2005) and future simulations (2081–2100) to estimate the large atmosphere-biosphere carbon fluxes and budget over the ABoVE domain (figure 2). We also add three observation-derived fluxes (GPP, RECO, and NEE) from the GBAF (Jung *et al* 2010) in the analysis for reference in the historical period. GBAF ABoVE domain estimated GPP is 2.68 PgC yr^{-1}, which corresponds to 2.23% of reference value global GPP, while GBAF ABoVE domain estimated RECO is 2.24 PgC yr^{-1}, which corresponds to 2.04% of reference value global RECO. GBAF ABoVE domain estimated NEE is −0.03 PgC yr^{-1}, which corresponds to 0.3% of the reference value global NEE.

In a single model, the carbon fluxes are expected to add up, but not in the ensemble member intercomparison. These numbers indicate the individual means of each carbon flux independently calculated across all models included in the ensemble members. The standard deviation of the means is shown in brackets next to their respective values.

The historical period CMIP5 ensemble member gives a GPP of 4.18 PgC yr^{-1}, which is revised downwards by the CMIP6 ensemble member to 3.28 PgC yr^{-1} for the same period, a reduction of 21.5% in GPP. Likewise, the historical period CMIP5 ensemble member gives a RECO of 3.55 PgC yr^{-1}, which is revised downwards by the CMIP6 ensemble member to 3.14 PgC yr^{-1} for the same period, a reduction of 11.5% in RECO. As a result, historical period CMIP5 ensemble member gives a NEE of −0.18 PgC yr^{-1}, which is revised upwards by the CMIP6 ensemble member to −0.12 PgC yr^{-1} for the same period, an increase of 33.3% in NEE. The overall reduction in fluxes is mostly due to the inclusion of the nitrogen cycle in CMIP6, lowering the absolute strength of the feedback parameters over land (Arora *et al* 2020). This suggests that if all next generations ESMs were to include the nutrient limitation (nitrogen and phosphorus) of photosynthesis and respiration, the spread across models will potentially be further reduced.

The carbon flux associated with DISTs was revised downwards for the historical period by the CMIP6 ensemble member (0.07 PgC yr^{-1}) in relation to the DIST carbon flux estimated by the CMIP5 ensemble member (0.11 PgC yr^{-1}), a total reduction of 57.1%. Adding all these fluxes together gives a budget NBP of 0.07 PgC yr^{-1} for both ensemble members, which defines the ABoVE domain as a carbon sink over the historical period.

For future scenarios, the CMIP5 ensemble member projects an increase in GPP of 74.7% (7.32 PgC yr^{-1}), while the CMIP6 ensemble member projects an increase in GPP of 98.4% (6.51 PgC yr^{-1}) with a much stronger CO_2 fertilization effect. Likewise, the CMIP5 ensemble member projects an increase in RECO of 72.1% (6.11 PgC yr^{-1}), while the CMIP6 ensemble member projects an increase in RECO of 88.2% (5.91 PgC yr^{-1}). Although the carbon emissions by DISTs is also projected to have a stronger increase according to the CMIP6 ensemble member (157%) versus the CMIP5 ensemble member (36.4%), the ABoVE domain is projected to be a

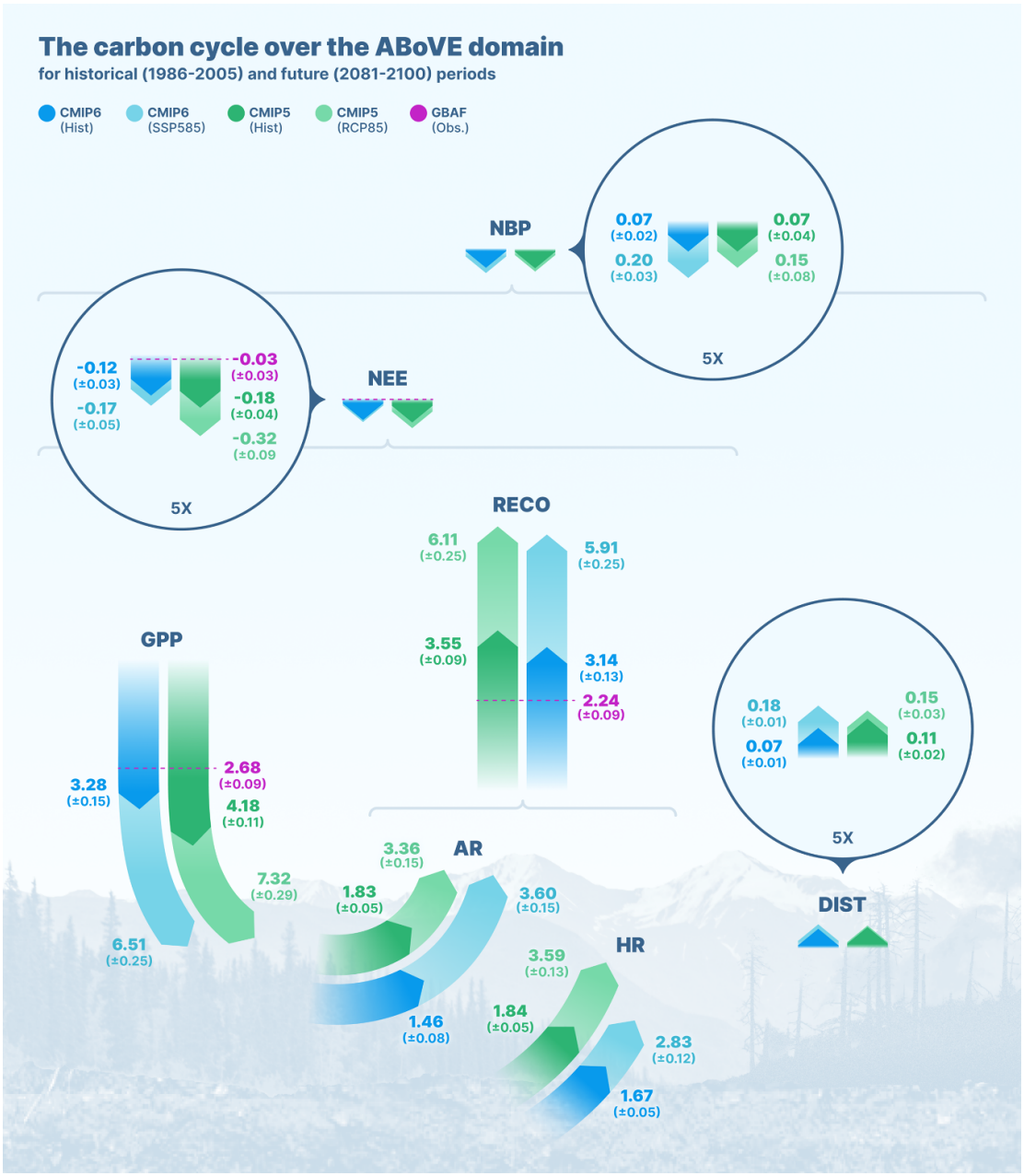

Figure 2. Atmosphere-biosphere carbon fluxes over the ABoVE domain for the historical period (1986–2005) and future (2081–2100) according to the CMIP5 and CMIP6 ensemble members. Three observation derived fluxes (GPP, RECO and NEE) from the Global Bio-Atmosphere Flux (GBAF) (Jung *et al* 2010) in the analysis for reference in the historical period. Arrows point to the direction (into or out of land) of the carbon flux. The standard deviation of the means is shown in brackets next to their respective values.

carbon sink by the end of the 21st century with a total carbon uptake of 0.20 PgC yr^{-1} in the CMIP6 and 0.15 PgC yr^{-1} in the CMIP5 simulations.

3.3. Persistent tipping point in NBP over the ABoVE domain in new generation ESMs

Under high emissions scenarios, a relative strengthening of global land carbon–climate feedbacks leads the terrestrial biosphere to shift from a carbon sink to a carbon source at some point after 2100 in all of the CMIP5 ESMs (IPCC 2007, Tokarska *et al* 2016). Likewise, Koven *et al* (2022) evaluated land carbon fluxes globally from 5 CMIP6 members until 2300 and found that terrestrial ecosystems are projected to switch from being a net sink to either a neutral state or a net source of carbon depending on the model and the scenario used in the projections. Nevertheless, Koven *et al* (2022) highlight that land models qualitatively disagree in the spatial patterns, the timing, and the magnitudes of the carbon responses to climate change. Therefore, the diverse potential for global and regional carbon cycle dynamics to change sign under different scenarios highlights the continued need for improved comprehension of the major drivers of terrestrial carbon cycle dynamics.

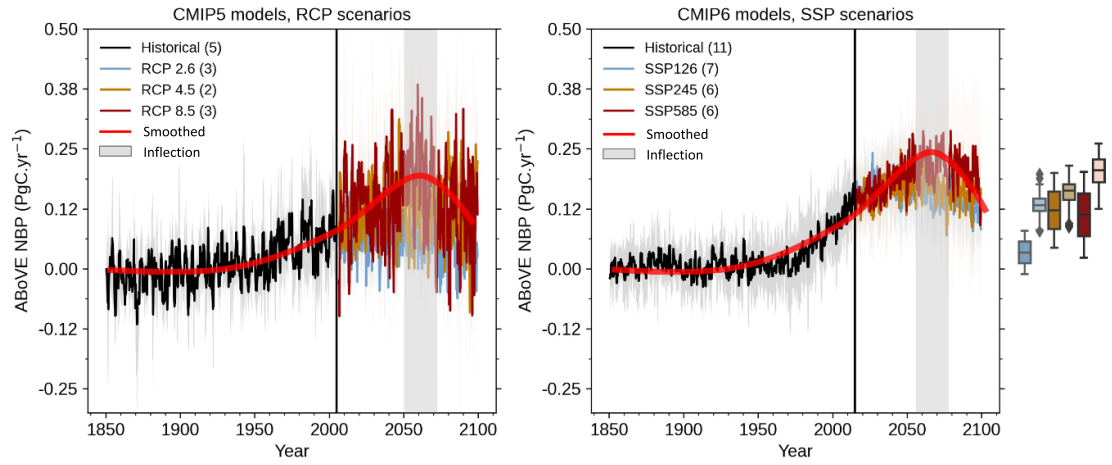

Figure 3. Net biome production (NBP) (mean and one standard deviation as shading) over the region of NASA's Arctic-Boreal vulnerability experiment (ABoVE) in North America from 1850 to 2100 for the RCP scenarios run by CMIP5 and the SSP scenarios run by CMIP6. The number of models is given in brackets. The box plots (mean, one standard deviation, and minimum to maximum range) are given for 2080–2099 for CMIP5 (dark colors) and CMIP6 (light colors). A smoothed line (red) is adjusted to the historical data and forcing 8.5 W m^{-2}. The 20 year window around the inflection point is shown in gray.

Although we have not directly evaluated climate data after 2100, we found that a tipping point on the NBP curve by 2050–2080 persists in North American Arctic-Boreal ecosystems too, despite minimized uncertainty in CMIP6 models (figure 3 box plot). However, the remaining large spread in ESM projections and the lack of model representation of fundamental mechanistic processes that may amplify or mitigate soil carbon losses on longer time scales (including microbial dynamics, permafrost, peatlands, and nutrients) lead to low confidence in the magnitude of global soil carbon losses with global warming (IPCC, 2007, 2021).

Nevertheless, both CMIP ensemble members across different carbon emission scenarios project a tipping point between 2050 and 2080. The carbon sink strength over the ABoVE domain starts to decrease during these years, indicating that sometime in the next century the North American Arctic-Boreal ecosystems will likely become a source of carbon to the atmosphere. This will amplify the local and global impacts of climate change already attributed to a local physical component, the permafrost (Natali *et al* 2019).

The reason for this tipping point in NBP over the ABoVE domain is that, although all the components of NBP are projected to increase throughout the 21st century (figure S2), the growth rate sum of both respiration terms (0.020 PgC yr^{-2} and 0.015 PgC yr^{-2} for autotrophic and heterotrophic respiration, respectively) plus DISTs (9×10^{-4} PgC yr^{-2}) is at least 15% larger than the growth rate of photosynthesis (0.020 PgC yr^{-2}) over the same period according to CMIP6. The rate of change related to RECO (and DISTs) is outpacing increases in GPP, which suggests that the thermal response on respiration from warming is greater than photosynthetic gains from CO_2 fertilization and longer, warmer growing seasons.

The tipping point in NBP identified in our analysis may be interpreted as simply due to the CO_2 emissions flattening out (representative concentration pathway (RCP 8.5)) or decreasing (SSP585) in future scenarios (Meinshausen *et al* 2020); however, this is proven not to be the case when evaluating individual carbon fluxes projections over the ABoVE domain (figure S2). All carbon fluxes over the ABoVE domain keep going up until at least 2100, i.e.after the CO_2 emissions flatten out (RCP 8.5) or decrease (SSP585), which indicates that climatic factors and not CO_2 are driving the carbon fluxes up. The mean NBP for the ABoVE region over the 20th and 21st century as simulated by the CMIP5 and CMIP6 models is shown in figure 3. The simulated 20th century net carbon flux is steeper in the CMIP6 model mean because the absolute values of land carbon-concentration feedback are larger, as also shown in Arora *et al* (2020). In addition, more CMIP6 models include a representation of the nitrogen cycle (table 1), which worked to reduce model spread despite the additional added complexity (Arora *et al* 2020). While the interannual variations are larger in CMIP5 models, these models make use of RCPs to determine the amount of warming that could occur by the end of the 21st century, by setting pathways for greenhouse gas concentrations, the SSPs set the stage on which reductions in emissions will—or will not—be reached. The model spread relative to the model mean change for each scenario is smaller for CMIP6 (figure 3 box plots), implying that these models present higher convergence in their projections than CMIP5. This suggests that despite more model complexity, the spread across land models is reduced in more recent versions.

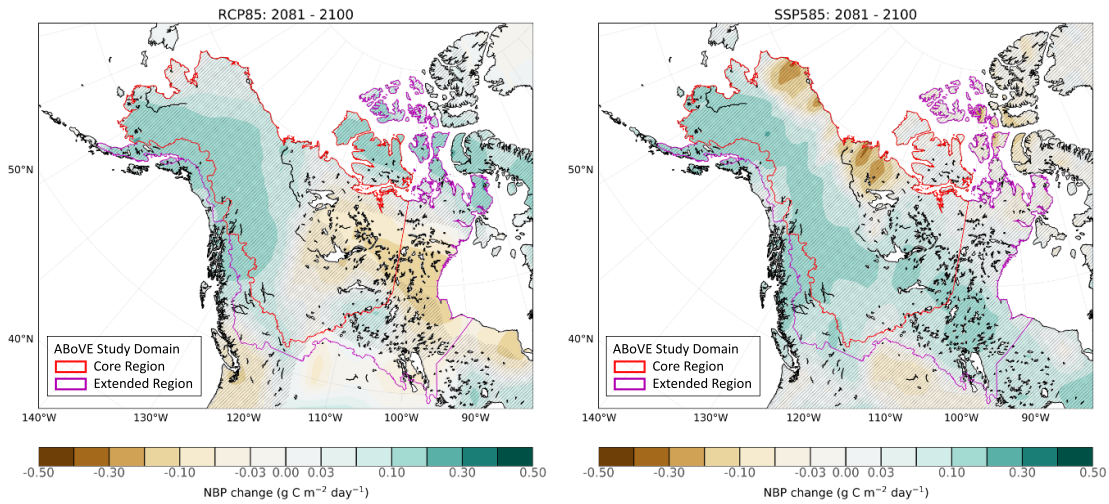

Figure 4. Multi-model mean NBP change (gCm^{-2} d^{-1}) for a 20 year time period centered around 2090, relative to 1986–2005, for CMIP5 (left) and CMIP6 (right). Stippling marks areas where the standard deviation of the model mean is 80% or less of the standard deviation of the interannual variability.

Despite disagreements in total carbon sink strength among CMIP5 and CMIP6 ensemble members, both CMIP versions agree that some areas of the ABoVE domain will indeed become stronger carbon sinks in the future relative to historical values. This indicates that the CO_2 fertilization effect of photosynthesis is predicted to overcome climate change impacts on respiration and other loss fluxes. Model mean patterns of NBP change for a 20 year time period centered around 2090, relative to 1986–2005, are shown in figure 4.

Although some areas are similar in CMIP5 and CMIP6, CMIP6 NBP is projected to increase in the South and West of the Hudson Bay, and decrease in northern Alaska, as well as the northern areas of Yukon and the Northwest territories. This is associated with less resilient land cover types, such as grasslands and open shrublands.

Tundra ecosystems are less resilient than boreal forests because of their low biodiversity (only 3% of the world's flora), low biomass (short and sparse vegetation), and low NPP (long and cold winters). In addition, permafrost makes it very difficult for roots to penetrate the soil, as well as slowing the decay of organic matter, which decreases the availability of nutrients (Scheffer *et al* 2012, Dial *et al* 2022). A robust increase in NBP is projected over southern Alaska and British Columbia across both model generations. This increase indicates a positive feedback in the productivity of evergreen needleleaf and mixed forests. Stippling on the maps is used to show model agreement locally, highlighting areas where the standard deviation of the model mean is 80% or less of the standard deviation of the interannual variability. For CMIP5 NBP change in figure 4, model agreement is not present in the South and West of the Hudson Bay or areas associated with mixed grasslands in the great plains. For CMIP6 NBP change in figure 4, stippling marks areas are present across the entire evaluated domain, highlighting also a spatial model convergence on top of an absolute one (figure 3).

4. Discussion

Modern model versions increase our confidence in prediction as more computational power, observations, and process understanding are available. CMIP6 predicts a stronger carbon sink in the ABoVE domain than previously predicted by CMIP5, and smaller spread across all scenarios (figure 3 box plots). Smaller model spread in land carbon fluxes over the ABoVE domain are primarily due to better representations of photosynthesis, respiration, and biomass, although clear improvements in soil carbon are still lacking (figure 1).

The Arctic-Boreal carbon cycle in CMIP6 represents more of the relevant processes with increased detail. For example, while GPP generally presents high ILAMB overall scores because the description of processes like photosynthesis generally relies on very well-established ecophysiology models (Farquhar *et al* 1980, Collatz *et al* 1992), other processes controlling the stocking of carbon in vegetation, like respiration, litterfall, and allocation lack a unifying or generally acceptable framework (Reichstein and Carvalhais 2019). Moreover, the way in which ESMs calculate permafrost—defined as ground where soil temperature remains at or below 0 °C continuously for at least 2 years (Black and Muller 1948, Guo and Wang 2016)—is directly linked to the representation of snow and soil physics of each individual model, rather than a newly implemented modeling feature, such permafrost thawing heterogeneous dynamics and nutrient cycling, for example. Previous studies

have evaluated permafrost from CMIP5 (Koven *et al* 2013, Slater *et al* 2017) and CMIP6 (Burke *et al* 2020) and found that the spread of simulated present-day permafrost area within the ensemble members is large and mainly caused by structural divergences in mechanistic processes representation of soils and snow within models.

Even though the model spread in CMIP5 and CMIP6 projections are similar or only slightly smaller in CMIP6, scientists have incorporated some of the missing processes (such as components of the nitrogen cycle, for example) into carbon cycle projections, so we are more confident that ESMs capture more of the relevant land surface processes. Nevertheless, ILAMB scores should be used with caution when demonstrating model improvement or ranking models in their performance (Collier *et al* 2018). Spatiotemporal GPP and LAI biases between CMIP5 and CMIP6 with FLUXCOM and MODIS indicate a general improvement of CMIP6 models over CMIP5 models. Higher relationship scores of GPP and LAI with precipitation, downward shortwave radiation, and temperature indicate not only a general improvement towards smaller biases with observations, but also a more accurate mechanist process representation as function of environmental variables in newer model versions.

Spatiotemporal GPP biases between CMIP5 and CMIP6 with FLUXCOM for the period from 1980 to 2014 are improved by approximately 30% in newer model versions, with especially accurate performance during spring (figure S4). For LAI, the spatiotemporal biases between CMIP5 and CMIP6 with MODIS for the period from 2000 to 2006 are improved by approximately 40% in newer model versions (figure S6). The climate sensitives of GPP and LAI are also improved in CMIP6 models as indicated by higher scores between reference datasets to their relationships to climatic variables diagnosed in the models (figures S5 and S7 in supporting information).

A persistent tipping point in the NBP curve by 2050–2080 is projected over the ABoVE domain despite minimized uncertainty in CMIP6 models (figure 3 box plot). The tipping point in the NBP growing curve over the ABoVE domain is not simply due to the CO_2 emissions flattening out (RCP 8.5) or decreasing (SSP585) in future scenarios, but rather a combination of different carbon fluxes with opposite signs growing at different rates, namely respiration terms plus DISTs being at least 15% larger than the growth rate of photosynthesis (figure S2). This indicates that climate change and not the CO_2 fertilization effect is causing this tipping point in the carbon cycle over the ABoVE domain. The rate of change related to RECO (and DISTs) outpaces carbon gains from GPP, which suggests that the thermal and moisture responses on respiration is larger than the photosynthetic gains from the CO_2 fertilization effect, as well as longer and warmer growing seasons.

In general, CMIP6 has higher ILAMB overall scores compared with CMIP5, although soil carbon is an exception. Initial attempts to model the relationships between soil carbon and climate factors were not successful to predict the uncertain effects of climate and land use change (Post *et al* 1982). These first models described soil carbon as being mainly controlled by evapotranspiration and precipitation rates, as well as plant functional types. However, it is now understood that soil carbon depends on a number of other mechanistic relationships with soil type, microbial communities, as well as species composition. Taken together, soil carbon uncertainties need to be addressed in the next generation of ESMs with greater emphasis of the modeling community by basing more off mechanistic science of the relationships driving soil and rhizospheric processes (Pallandt *et al* 2022).

Soil carbon and soil carbon turnover time are an exception to the general model improvement from CMIP5 to CMIP6 and have a lower benchmarking score for CMIP6 than for CMIP5 (figure 1). Although it is usually the case to use ILAMB overall scores to backup conclusions about model improvement, a more detailed evaluation analysis of the component metrics that determine the overall scores is required (Collier *et al* 2018, Bonan *et al* 2019), especially because ILAMB analysis assigns relative weights to each dataset to qualitatively account for uncertainty in the datasets themselves and multiple statistical metrics (see equation (1)). Moreover, previous studies have shown that ESMs cannot reproduce soil carbon under current climate (Todd-Brown *et al* 2013, 2014, Luo *et al* 2015) or regionally, as well as global carbon soil datasets present large discrepancies (Tifafi *et al* 2018, Crowther *et al* 2019) making it very challenging to appropriately conduct a model benchmarking. Global overall scores for soil turnover time also indicate a degradation in model performance in CMIP6 over CMIP5 (figure S9).

Model discrepancies and lower overall scores in ILAMB highlight soil carbon assumptions that deserve further investigations, especially regarding how ecosystems are likely responding to climate change and shifts in resource availability (Giorgi 2006, Wieder *et al* 2019, Braghiere *et al* 2022). Future model development endeavors should carefully consider rhizospheric and soil processes, for example the inclusion of nutrient dynamics into ESMs could help constrain the CO_2 fertilization effect (Norby *et al* 2010, Reich and Hobbie 2013, Terrer *et al* 2018, Braghiere *et al* 2022).

Although previous studies have hypothesized that rising temperatures may increase soil carbon losses through decreased soil turnover times mainly due to increased heterotrophic respiration, especially in high latitudes (Davidson and Janssens 2006, Koven

et al 2011, Bond-Lamberty *et al* 2018), other effects like aggregate formation and mineral–organic interactions could actually stabilize soil carbon, limiting the loss responses to increased temperature (Dungait *et al* 2012, Han Weng *et al* 2017).

Decomposition model structures generally use first-order decay kinetics and lack to represent microbial traits, but they could be updated to include microbial priming effects, as well as mineral–soil organic carbon interactions (Todd-Brown *et al* 2013, Wan and Crowther 2022). In addition, physical processes like erosion, soil creep, as well as river transport of carbon and sediments are typically not represented in ESMs, but they can be critical for carbon cycling (Resplandy *et al* 2018), especially from permafrost thawing.

Often experimental manipulations can indicate unanticipated ecosystem responses from theoretical expectations or previous observations (Melillo *et al* 2017, Reich *et al* 2018), but these experiments can be expensive and demanding, which limit their spatial and temporal coverage. In order to expand scientific possibilities, modern ESMs should be enabled to make direct use of new observations from spacecraft in orbit allowing an estimation of carbon cycle variables, linking eddy covariance sites with much higher spatial coverages (Schimel and Schneider 2019, Braghiere *et al* 2021a).

The challenge remains on how to link above canopy measurable signatures to underground rhizospheric mechanisms, which depends upon the development of new theory to address previously unobserved processes. Hyperspectral datasets seem highly promising in deriving a wide range of unique constraints on plant functional traits that can be linked to the rhizosphere (Singh *et al* 2015, Butler *et al* 2017, Sousa *et al* 2021). As a way forward, scientists should be able to bridge different process-based model scales and modeling parametric decisions (Shi *et al* 2018, Braghiere *et al* 2020a, Wang *et al* 2021), as well as applying machine learning tools to spatially and temporally limited data to improve understanding about complex processes in which current models have little to no mechanistic ways to represent (Bloom *et al* 2016, Braghiere *et al* 2020b).

5. Conclusion

The rapid warming of the Arctic-Boreal zone is expected to shift current states of the biosphere indefinitely, moving the Earth system into new, and possibly irreversible states (Lenton 2012, Seidl *et al* 2017). Future NBP projections indicate narrower model spread for CMIP6, while both CMIPs indicate a tipping point in the NBP growing curve by 2050–2080 suggesting that, if the carbon sink strength keeps declining throughout the 21st century, the Arctic-Boreal ecosystems in North America will highly likely become a carbon source in the next century.

In general, simulated carbon cycle variables from CMIP6 better agree with observations than those from CMIP5 for the globe and the ABoVE domain with an exception for soil carbon and turnover rate (figure 1). While processes like photosynthesis rely on well-established ecophysiology models (Farquhar *et al* 1980, Collatz *et al* 1992) and present improvements in relationship to climatic variables, soil carbon lacks a generally acceptable description and processes understanding (Reichstein and Carvalhais 2019), which can be alleviated with more experimental manipulations, observations, and newer modeling paradigms.

Data availability statement

The data that support the findings of this study are openly available. The CMIP6 data simulations performed by various modeling groups are available from the CMIP6 archive (https://esgf-node.llnl.gov/search/cmip6). The ILAMB package can be downloaded from (https://github.com/rubisco-sfa/ILAMB). All ILAMB plots are available from (https://braghiere.github.io/).

Acknowledgments

This study was part of the NASA Arctic-Boreal Vulnerability Experiment (ABoVE). RKB and JBF were supported through funding from Phase 2 of NASA ABoVE (NNX15AV77A). Part of this research was carried out at the Jet Propulsion Laboratory, California Institute of Technology, under a contract with the National Aeronautics and Space Administration (80NM0018D004). California Institute of Technology. Government sponsorship acknowledged. This research used resources of the NASA ABoVE program. We acknowledge support from the NASA ABoVE (incl. 80NSSC22K1245, NNX17AD69A) and ILAMB communities. This work was supported in part by Resnick Sustainability Institute.

Author contribution

RKB planned and designed the research. JBF supervised and acquired funding. RKB performed the research, data analysis, collection, and interpretation, as well as wrote the original draft and final manuscript with input from all authors.

Conflict of interest

The authors declare no competing interests.

ORCID iDs

Renato K Braghiere https://orcid.org/0000-0002-7722-717X
Joshua B Fisher https://orcid.org/0000-0003-4734-9085

Kimberley R Miner https://orcid.org/0000-0002-1006-1283
Charles E Miller https://orcid.org/0000-0002-9380-4838
John R Worden https://orcid.org/0000-0003-0257-9549
David S Schimel https://orcid.org/0000-0003-3473-8065
Christian Frankenberg https://orcid.org/0000-0002-0546-5857

References

Adler R *et al* 2018 The Global Precipitation Climatology Project (GPCP) monthly analysis (new version 2.3) and a review of 2017 *Glob. Precip. Atmos.* **9** 138
Ahlström A *et al* 2015 The dominant role of semi-arid ecosystems in the trend and variability of the land CO_2 sink *Science* **348** 895–9
Anav A *et al* 2015 Spatiotemporal patterns of terrestrial gross primary production: a review *Rev. Geophys.* **53** 785–818
Anav A, Friedlingstein P, Kidston M, Bopp L, Ciais P, Cox P, Jones C, Jung M, Myneni R and Zhu Z 2013 Evaluating the land and ocean components of the global carbon cycle in the CMIP5 Earth system models *J. Clim.* **26** 6801–43
Armstrong Mckay D I, Staal A, Abrams J F, Winkelmann R, Sakschewski B, Loriani S, Fetzer I, Cornell S E, Rockström J and Lenton T M 2022 Exceeding 1.5 °C global warming could trigger multiple climate tipping points *Science* **377** eabn7950
Arora V K *et al* 2020 Carbon-concentration and carbon-climate feedbacks in CMIP6 models and their comparison to CMIP5 models *Biogeosciences* **17** 4173–222
Arora V K and Boer G J 2005 A parameterization of leaf phenology for the terrestrial ecosystem component of climate models *Glob. Change Biol.* **11** 39–59
Arora V K, Scinocca J F, Boer G J, Christian J R, Denman K L, Flato G M, Kharin V V, Lee W G and Merryfield W J 2011 Carbon emission limits required to satisfy future representative concentration pathways of greenhouse gases *Geophys. Res. Lett.* **38**
Bentsen M *et al* 2013 The Norwegian Earth system model, NorESM1-M—part 1: description and basic evaluation of the physical climate *Geosci. Model Dev.* **6** 687–720
Berner L T *et al* 2020 Summer warming explains widespread but not uniform greening in the Arctic tundra biome *Nat. Commun.* **11** 1–12
Best M J *et al* 2011 The Joint UK Land Environment Simulator (JULES), model description. Part 1: energy and water fluxes *Geosci. Model Dev.* **4** 677–99
Bi D *et al* 2020 Configuration and spin-up of ACCESS-CM2, the new generation Australian Community Climate and Earth system simulator coupled model *J. South. Hemisphere Earth Syst. Sci.* **70** 225–51
Black R F and Muller S W 1948 Permafrost or permanently frozen ground and related engineering problems *Geogr. Rev* **38** 686
Blackard J A *et al* 2008 Mapping U.S. forest biomass using nationwide forest inventory data and moderate resolution information *Remote Sens. Environ.* **112** 1658–77
Bloom A A, Exbrayat J-F, van der Velde I R, Feng L and Williams M 2016 The decadal state of the terrestrial carbon cycle: global retrievals of terrestrial carbon allocation, pools, and residence times *Proc. Natl Acad. Sci.* **113** 1285–90
Bonan G B, Lombardozzi D L, Wieder W R, Oleson K W, Lawrence D M, Hoffman F M and Collier N 2019 Model structure and climate data uncertainty in historical simulations of the terrestrial carbon cycle (1850–2014) *Glob. Biogeochem. Cycles* **33** 1310–26
Bond-Lamberty B, Bailey V L, Chen M, Gough C M and Vargas R 2018 Globally rising soil heterotrophic respiration over recent decades *Nature* **560** 80–83
Boucher O *et al* 2020 Presentation and evaluation of the IPSL-CM6A-LR climate model *J. Adv. Model. Earth Syst.* **12** e2019MS002010
Braghiere R K *et al* 2021a Accounting for canopy structure improves hyperspectral radiative transfer and sun-induced chlorophyll fluorescence representations in a new generation *Earth Syst. Model Remote Sens. Environ.* **261** 112497
Braghiere R K *et al* 2021b Mycorrhizal distributions impact global patterns of carbon and nutrient cycling *Geophys. Res. Lett.* **48** e2021GL094514
Braghiere R K, Fisher J B, Allen K, Brzostek E, Shi M, Yang X, Ricciuto D M, Fisher R A, Zhu Q and Phillips R P 2022 Modeling global carbon costs of plant nitrogen and phosphorus acquisition *J. Adv. Model. Earth Syst.* **14** e2022MS003204
Braghiere R K, Gérard F, Evers J B, Pradal C and Pagès L 2020a Simulating the effects of water limitation on plant biomass using a 3D functional–structural plant model of shoot and root driven by soil hydraulics *Ann. Bot.* **126** 713–28
Braghiere R K, Quaife T, Black E, He L and Chen J M 2019 Underestimation of global photosynthesis in Earth system models due to representation of vegetation structure *Glob. Biogeochem. Cycles* **33** 1358–69
Braghiere R K, Yamasoe M A, Évora Do Rosário N M, Ribeiro da Rocha H, de Souza Nogueira J and de Araújo A C 2020b Characterization of the radiative impact of aerosols on CO2 and energy fluxes in the Amazon deforestation arch using artificial neural networks *Atmos. Chem. Phys.* **20** 3439–58
Buermann W, Parida B, Jung M, MacDonald G M, Tucker C J and Reichstein M 2014 Recent shift in Eurasian boreal forest greening response may be associated with warmer and drier summers *Geophys. Res. Lett.* **41** 1995–2002
Burke E J, Zhang Y and Krinner G 2020 Evaluating permafrost physics in the coupled model intercomparison project 6 (CMIP6) models and their sensitivity to climate change *Cryosphere* **14** 3155–74
Butler E E *et al* 2017 Mapping local and global variability in plant trait distributions *Proc. Natl Acad. Sci. USA* **114** E10937–46
Ciais P *et al* 2019 Five decades of northern land carbon uptake revealed by the interhemispheric CO2 gradient *Nature* **568** 221–5
Clark D B *et al* 2011 The Joint UK Land Environment Simulator (JULES), model description. Part 2: carbon fluxes and vegetation dynamics *Geosci. Model Dev.* **4** 701–22
Claverie M *et al* 2016 A 30+ year AVHRR LAI and FAPAR climate data record: algorithm description and validation *Remote Sens.* **8** 263
Collatz G, Ribas-Carbo M and Berry J 1992 Coupled photosynthesis-stomatal conductance model for leaves of C4 plants *Funct. Plant Biol.* **19** 519
Collier N, Hoffman F M, Lawrence D M, Keppel-Aleks G, Koven C D, Riley W J, Mu M and Randerson J T 2018 The International Land Model Benchmarking (ILAMB) system: design, theory, and implementation *J. Adv. Model. Earth Syst.* **10** 2731–54
Crowther T W, Thomas S M, Maynard D S, Baldrian P, Covey K, Frey S D, Van Diepen L T A and Bradford M A 2015 Biotic interactions mediate soil microbial feedbacks to climate change *Proc. Natl Acad. Sci. USA* **112** 7033–8
Crowther T W, van den Hoogen J, Wan J, Mayes M A, Keiser A D, Mo L, Averill C and Maynard D S 2019 The global soil community and its influence on biogeochemistry *Science* **365**
Danabasoglu G *et al* 2020 The community Earth system model version 2 (CESM2) *J. Adv. Model. Earth Syst.* **12** e2019MS001916
Davidson E A and Janssens I A 2006 Temperature sensitivity of soil carbon decomposition and feedbacks to climate change *Nature* **440** 165–73

De Kauwe M G, Disney M I, Quaife T, Lewis P and Williams M 2011 An assessment of the MODIS collection 5 leaf area index product for a region of mixed coniferous forest *Remote Sens. Environ.* **115** 767–80

de Vrese P and Brovkin V 2021 Timescales of the permafrost carbon cycle and legacy effects of temperature overshoot scenarios *Nat. Commun.* **12** 1–13

De Vrese P, Stacke T, Kleinen T and Brovkin V 2021 Diverging responses of high-latitude co2 and ch4 emissions in idealized climate change scenarios *Cryosphere* **15** 1097–130

Delire C *et al* 2020 The global land carbon cycle simulated with ISBA-CTRIP: improvements over the last decade *J. Adv. Model. Earth Syst.* **12** e2019MS001886

Dial R J, Maher C T, Hewitt R E and Sullivan P F 2022 Sufficient conditions for rapid range expansion of a boreal conifer *Nature* **603** 546–51

Dufresne J-L *et al* 2013 Climate change projections using the IPSL-CM5 Earth system model: from CMIP3 to CMIP5 *Clim. Dyn.* **40** 2123–65

Dungait J A J, Hopkins D W, Gregory A S and Whitmore A P 2012 Soil organic matter turnover is governed by accessibility not recalcitrance *Glob. Change Biol.* **18** 1781–96

Dunne J P *et al* 2020 The GFDL Earth system model version 4.1 (GFDL-ESM 4.1): overall coupled model description and simulation characteristics *J. Adv. Model. Earth Syst.* **12** e2019MS002015

Eyring V, Bony S, Meehl G A, Senior C A, Stevens B, Stouffer R J and Taylor K E 2016 Overview of the coupled model intercomparison project phase 6 (CMIP6) experimental design and organization *Geosci. Model Dev.* **9** 1937–58

Farquhar G D, Caemmerer S and Berry J A 1980 A biochemical model of photosynthetic CO2 assimilation in leaves of C3 species *Planta* **149** 78–90

Fer I *et al* 2021 Beyond ecosystem modeling: a roadmap to community cyberinfrastructure for ecological data-model integration *Glob. Change Biol.* **27** 13–26

Fisher J B *et al* 2018 Missing pieces to modeling the Arctic-Boreal puzzle *Environ. Res. Lett.* **13** 020202

Fisher R A *et al* 2018 Vegetation demographics in Earth system models: a review of progress and priorities *Glob. Change Biol.* **24** 35–54

Francis J A, Vavrus S J and Cohen J 2017 Amplified Arctic warming and mid-latitude weather: new perspectives on emerging connections *Wiley Interdiscip. Rev. Clim. Change* **8** e474

Giorgetta M A *et al* 2013 Climate and carbon cycle changes from 1850 to 2100 in MPI-ESM simulations for the coupled model intercomparison project phase 5 *J. Adv. Model. Earth Syst.* **5** 572–97

Giorgi F 2006 Climate change hot-spots *Geophys. Res. Lett.* **33** 8707

Guo D and Wang H 2016 CMIP5 permafrost degradation projection: a comparison among different regions *J. Geophys. Res. Atmos.* **121** 4499–517

Han Weng Z *et al* 2017 Biochar built soil carbon over a decade by stabilizing rhizodeposits *Nat. Clim. Change* **7** 371–6

Harris I, Jones P D, Osborn T J and Lister D H 2014 Updated high-resolution grids of monthly climatic observations—the CRU TS3.10 dataset *Int. J. Climatol.* **34** 623–42

Hausfather Z, Marvel K, Schmidt G A, Nielsen-Gammon J W and Zelinka M 2022 Climate simulations: recognize the 'hot model' problem *Nature* **605** 26–29

Hawkins E and Sutton R 2009 The potential to narrow uncertainty in regional climate predictions *Bull. Am. Meteorol. Soc.* **90** 1095–107

Hayes D J, McGuire A D, Kicklighter D W, Gurney K R, Burnside T J and Melillo J M 2011 Is the northern high-latitude land-based CO2 sink weakening? *Glob. Biogeochem. Cycles* **25**

Hinzman L D, Deal C J, Mcguire A D, Mernild S H, Polyakov I V and Walsh J E 2013 Trajectory of the Arctic as an integrated system *Ecol. Appl.* **23** 1837–68

Hoffman F M *et al* 2017 *2016 International Land Model Benchmarking (ILAMB) Workshop Report* available at: www.osti.gov/servlets/purl/1330803/

Hugelius G *et al* 2013a A new data set for estimating organic carbon storage to 3 m depth in soils of the northern circumpolar permafrost region *Earth Syst. Sci. Data* **5** 393–402

Hugelius G, Tarnocai C, Broll G, Canadell J G, Kuhry P and Swanson D K 2013b The northern circumpolar soil carbon database: spatially distributed datasets of soil coverage and soil carbon storage in the northern permafrost regions *Earth Syst. Sci. Data* **5** 3–13

Huntzinger D N *et al* 2020 Evaluation of simulated soil carbon dynamics in Arctic-Boreal ecosystems *Environ. Res. Lett.* **15** 025005

Hurtt G C *et al* 2011 Harmonization of land-use scenarios for the period 1500–2100: 600 years of global gridded annual land-use transitions, wood harvest, and resulting secondary lands *Clim. Change* **109** 117

Hurtt G C *et al* 2020 Harmonization of global land use change and management for the period 850–2100 (LUH2) for CMIP6 *Geosci. Model Dev.* **13** 5425–64

Intergovernmental Panel on Climate Change 2014 *Climate Change 2013—The Physical Science Basis* (Cambridge: Cambridge University Press) available at: http://ebooks.cambridge.org/ref/id/CBO9781107415324

IPCC 2007 *Climate Change 2007—The Physical Science Basis: Working Group I Contribution to the Fourth Assessment Report of the IPCC (Climate Change 2007)* ed S Solomon *et al* (Cambridge: Cambridge University Press)

Ito A and Oikawa T 2002 A simulation model of the carbon cycle in land ecosystems (Sim-CYCLE): a description based on dry-matter production theory and plot-scale validation *Ecol. Modell.* **151** 143–76

Ito G, Romanou A, Kiang N Y, Faluvegi G, Aleinov I, Ruedy R, Russell G, Lerner P, Kelley M and Lo K 2020 Global carbon cycle and climate feedbacks in the NASA GISS ModelE2.1 *J. Adv. Model. Earth Syst.* **12** e2019MS002030

Iversen T *et al* 2013 The Norwegian Earth system model, NorESM1-M—part 2: climate response and scenario projections *Geosci. Model Dev.* **6** 389–415

Jian J *et al* 2022 Historically inconsistent productivity and respiration fluxes in the global terrestrial carbon cycle *Nat. Commun.* **131** 1–9 available at: www.nature.com/articles/s41467-022-29391-5

Jung M *et al* 2010 Recent decline in the global land evapotranspiration trend due to limited moisture supply *Nature* **467** 951–4

Jung M *et al* 2020 Scaling carbon fluxes from eddy covariance sites to globe: synthesis and evaluation of the FLUXCOM approach *Biogeosciences* **17** 1343–65

Jung M, Koirala S, Weber U, Ichii K, Gans F, Camps-Valls G, Papale D, Schwalm C, Tramontana G and Reichstein M 2019 The FLUXCOM ensemble of global land-atmosphere energy fluxes *Sci. Data* **6** 1–14

Kato S, Rose F G, Rutan D A, Thorsen T J, Loeb N G, Doelling D R, Huang X, Smith W L, Su W and Ham S-H 2018 Surface irradiances of edition 4.0 clouds and the Earth's radiant energy system (CERES) energy balanced and filled (EBAF) data product *J. Clim.* **31** 4501–27

Keenan T F *et al* 2014 Net carbon uptake has increased through warming-induced changes in temperate forest phenology *Nat. Clim. Change* **4** 598–604

Knorr W 2000 Annual and interannual CO2 exchanges of the terrestrial biosphere: process-based simulations and uncertainties *Glob. Ecol. Biogeogr.* **9** 225–52

Knutti R and Sedláček J 2013 Robustness and uncertainties in the new CMIP5 climate model projections *Nat. Clim. Change* **3** 369–73

Koven C D *et al* 2022 Multi-century dynamics of the climate and carbon cycle under both high and net negative emissions scenarios *Earth Syst. Dyn.* **13** 885–909

Koven C D, Chambers J Q, Georgiou K, Knox R, Negron-Juarez R, Riley W J, Arora V K, Brovkin V, Friedlingstein P and Jones C D 2015 Controls on terrestrial carbon feedbacks by productivity versus turnover in the CMIP5 Earth system models *Biogeosciences* **12** 5211–28

Koven C D, Hugelius G, Lawrence D M and Wieder W R 2017 Higher climatological temperature sensitivity of soil carbon in cold than warm climates *Nat. Clim. Change* **7** 817–22

Koven C D, Riley W J and Stern A 2013 Analysis of permafrost thermal dynamics and response to climate change in the CMIP5 Earth system models *J. Clim.* **26** 1877–900

Koven C D, Ringeval B, Friedlingstein P, Ciais P, Cadule P, Khvorostyanov D, Krinner G and Tarnocai C 2011 Permafrost carbon-climate feedbacks accelerate global warming *Proc. Natl Acad. Sci. USA* **108** 14769–74

Kowalczyk E, Stevens L, Law R, Dix M, Wang Y, Harman I, Haynes K, Srbinovsky J, Pak B and Ziehn T 2013 The land surface model component of ACCESS: description and impact on the simulated surface climatology *Aust. Meteorol. Oceanogr. J.* **63** 65–82

Krinner G, Viovy N, de Noblet-ducoudré N, Ogée J, Polcher J, Friedlingstein P, Ciais P, Sitch S and Prentice I C 2005 A dynamic global vegetation model for studies of the coupled atmosphere-biosphere system *Glob. Biogeochem. Cycles* **19** 1–33

Lawrence D M *et al* 2019 The community land model version 5: description of new features, benchmarking, and impact of forcing uncertainty *J. Adv. Model. Earth Syst.* **11** 4245–87

Lawrence J, Popova E, Yool A and Srokosz M 2015 On the vertical phytoplankton response to an ice-free Arctic Ocean *J. Geophys. Res. Ocean* **120** 8571–82

Lenton T M 2012 Arctic climate tipping points *AMBIO* **41** 10–22

Lenton T M, Held H, Kriegler E, Hall J W, Lucht W, Rahmstorf S and Schellnhuber H J 2008 Tipping elements in the Earth's climate system *Proc. Natl Acad. Sci. USA* **105** 1786–93

Li W, Zhang Y, Shi X, Zhou W, Huang A, Mu M, Qiu B and Ji J 2019 Development of land surface model BCC_AVIM2.0 and its preliminary performance in LS3MIP/CMIP6 *J. Meteorol. Res.* **33** 851–69

Loeb N G, Doelling D R, Wang H, Su W, Nguyen C, Corbett J G, Liang L, Mitrescu C, Rose F G and Kato S 2018 Clouds and the Earth's radiant energy system (CERES) energy balanced and filled (EBAF) top-of-atmosphere (TOA) edition-4.0 data product *J. Clim.* **31** 895–918

Lovenduski N S and Bonan G B 2017 Reducing uncertainty in projections of terrestrial carbon uptake *Environ. Res. Lett.* **12** 044020

Luo Y, Keenan T F and Smith M 2015 Predictability of the terrestrial carbon cycle *Glob. Change Biol.* **21** 1737–51

Mack M C, Schuur E A G, Bret-Harte M S, Shaver G R and Chapin F S 2004 Ecosystem carbon storage in arctic tundra reduce by long-term nutrient fertilization *Nature* **431** 440–3

Martin G M *et al* 2011 The HadGEM2 family of met office unified model climate configurations *Geosci. Model Dev.* **4** 723–57

Masson-Delmotte V *et al* 2021 IPCC, 2021: Climate Change 2021: The Physical Science Basis. Contribution of Working Group I to the Sixth Assessment Report of the Intergovernmental Panel on Climate Change https://doi.org/10.1038/s41597-021-00916-9

Mauritsen T *et al* 2019 Developments in the MPI-M Earth system model version 1.2 (MPI-ESM1.2) and its response to increasing CO2 *J. Adv. Model. Earth Syst.* **11** 998–1038

McGuire A D *et al* 2012 An assessment of the carbon balance of Arctic tundra: comparisons among observations, process models, and atmospheric inversions *Biogeosciences* **9** 3185–204

McGuire A D *et al* 2018 Dependence of the evolution of carbon dynamics in the northern permafrost region on the trajectory of climate change *Proc. Natl Acad. Sci. USA* **115** 3882–7

Meinshausen M *et al* 2020 The shared socio-economic pathway (SSP) greenhouse gas concentrations and their extensions to 2500 *Geosci. Model Dev.* **13** 3571–605

Mekonnen Z A *et al* 2021 Arctic tundra shrubification: a review of mechanisms and impacts on ecosystem carbon balance *Environ. Res. Lett.* **16** 053001

Melillo J M, Frey S D, DeAngelis K M, Werner W J, Bernard M J, Bowles F P, Pold G, Knorr M A and Grandy A S 2017 Long-term pattern and magnitude of soil carbon feedback to the climate system in a warming world *Science* **358** 101–5

Miner K R, Turetsky M R, Malina E, Bartsch A, Tamminen J, McGuire A D, Fix A, Sweeney C, Elder C D and Miller C E 2022 Permafrost carbon emissions in a changing Arctic *Nat. Rev. Earth Environ.* **3** 55–67

Nachtergaele F *et al* 2012 Harmonized World Soil Database version 1.2. Food and Agriculture Organization of the United Nations (FAO). *19th World Congr. Soil Sci. Soil Solut. a Chang. World*

Natali S M *et al* 2019 Large loss of CO2 in winter observed across the northern permafrost region *Nat. Clim. Change* **9** 852–7

Natali S M, Schuur E A G and Rubin R L 2012 Increased plant productivity in Alaskan tundra as a result of experimental warming of soil and permafrost *J. Ecol.* **100** 488–98

Norby R J, Warren J M, Iversen C M, Medlyn B E and McMurtrie R E 2010 CO2 enhancement of forest productivity constrained by limited nitrogen availability *Proc. Natl Acad. Sci. USA* **107** 19368–73

Ø S *et al* 2020 Overview of the Norwegian Earth system model (NorESM2) and key climate response of CMIP6 DECK, historical, and scenario simulations *Geosci. Model Dev.* **13** 6165–200

Pallandt M, Ahrens B, Koirala S, Lange H, Reichstein M, Schrumpf M and Zaehle S 2022 Vertically divergent responses of SOC decomposition to soil moisture in a changing climate *J. Geophys. Res. Biogeosci.* **127** e2021JG006684

Park H and Jeong S 2021 Leaf area index in Earth system models: how the key variable of vegetation seasonality works in climate projections *Environ. Res. Lett.* **16** 034027

Pastorello G *et al* 2020 The FLUXNET2015 dataset and the ONEFlux processing pipeline for eddy covariance data *Sci. Data* **7** 1–27

Post W M, Emanuel W R, Zinke P J and Stangenberger A G 1982 Soil carbon pools and world life zones *Nature* **298** 156–9

Previdi M, Smith K L and Polvani L M 2021 Arctic amplification of climate change: a review of underlying mechanisms *Environ. Res. Lett.* **16** 093003

Raddatz T J, Reick C H, Knorr W, Kattge J, Roeckner E, Schnur R, Schnitzler K G, Wetzel P and Jungclaus J 2007 Will the tropical land biosphere dominate the climate-carbon cycle feedback during the twenty-first century? *Clim. Dyn.* **29** 565–74

Rantanen M, Karpechko A Y, Lipponen A, Nordling K, Hyvärinen O, Ruosteenoja K, Vihma T and Laaksonen A 2022 The Arctic has warmed nearly four times faster than the globe since 1979 *Commun. Earth Environ.* **3** 168

Reich P B and Hobbie S E 2013 Decade-long soil nitrogen constraint on the CO2 fertilization of plant biomass *Nat. Clim. Change* **3** 278–82

Reich P B, Hobbie S E, Lee T D and Pastore M A 2018 Unexpected reversal of C_3 versus C_4 grass response to elevated CO_2 during a 20-year field experiment *Science* **360** 317–20

Reichstein M and Carvalhais N 2019 Aspects of forest biomass in the Earth system: its role and major unknowns *Surv. Geophys.* **40** 693–707

Resplandy L, Keeling R F, Rödenbeck C, Stephens B B, Khatiwala S, Rodgers K B, Long M C, Bopp L and Tans P P 2018 Revision of global carbon fluxes based on a reassessment of oceanic and riverine carbon transport *Nat. Geosci.* **11** 504–9

Saatchi S S et al 2011 Benchmark map of forest carbon stocks in tropical regions across three continents Proc. Natl Acad. Sci. 108 9899–904
Sato H, Itoh A and Kohyama T 2007 SEIB–DGVM: a new dynamic global vegetation model using a spatially explicit individual-based approach Ecol. Modelling 200 279–307
Scheffer M, Hirota M, Holmgren M, Van Nes E H and Chapin F S 2012 Thresholds for boreal biome transitions Proc. Natl Acad. Sci. USA 109 21384–9
Schimel D and Schneider F D 2019 Flux towers in the sky: global ecology from space New Phytol. 224 570–84
Schimel D, Stephens B B and Fisher J B 2015 Effect of increasing CO 2 on the terrestrial carbon cycle Proc. Natl Acad. Sci. 112 436–41
Schuur E A G et al 2015 Climate change and the permafrost carbon feedback Nature 520 171–9
Seidl R et al 2017 Forest disturbances under climate change Nat. Clim. Change 7 395–402
Sellar A A et al 2019 UKESM1: description and evaluation of the U.K. Earth system model J. Adv. Model. Earth Syst. 11 4513–58
Shao P, Zeng X, Sakaguchi K, Monson R K and Zeng X 2013 Terrestrial carbon cycle: climate relations in eight CMIP5 Earth system models J. Clim. 26 8744–64
Shevliakova E, Pacala S W, Malyshev S, Hurtt G C, Milly P C D, Caspersen J P, Sentman L T, Fisk J P, Wirth C and Crevoisier C 2009 Carbon cycling under 300 years of land use change: importance of the secondary vegetation sink Glob. Biogeochem. Cycles 23
Shi Z, Crowell S, Luo Y and Moore B 2018 Model structures amplify uncertainty in predicted soil carbon responses to climate change Nat. Commun. 9 1–11
Singh A, Serbin S P, McNeil B E, Kingdon C C and Townsend P A 2015 Imaging spectroscopy algorithms for mapping canopy foliar chemical and morphological traits and their uncertainties Ecol. Appl. 25 2180–97
Slater A G and Lawrence D M 2013 Diagnosing present and future permafrost from climate models J. Clim. 26 5608–23
Slater A G, Lawrence D M and Koven C D 2017 Process-level model evaluation: a snow and heat transfer metric Cryosphere 11 989–96
Sousa D et al 2021 Tree canopies reflect mycorrhizal composition Geophys. Res. Lett. 48 e2021GL092764
Steffen W, Noble I, Canadell J, Apps M, Schulze E-D and Jarvis P G 1998 The terrestrial carbon cycle: implications for the kyoto protocol Science 280 1393–4
Stofferahn E, Fisher J B, Hayes D J, Schwalm C R, Huntzinger D N, Hantson W, Poulter B and Zhang Z 2019 The Arctic-Boreal vulnerability experiment model benchmarking system Environ. Res. Lett. 14 055002
Swart N C et al 2019 The Canadian Earth system model version 5 (CanESM5.0.3) Geosci. Model Dev. 12 4823–73
Taylor K E, Stouffer R J and Meehl G A 2012 An overview of CMIP5 and the experiment design Bull. Am. Meteorol. Soc. 93 485–98
Terrer C, Vicca S, Stocker B D, Hungate B A, Phillips R P, Reich P B, Finzi A C and Prentice I C 2018 Ecosystem responses to elevated CO 2 governed by plant-soil interactions and the cost of nitrogen acquisition New Phytol. 217 507–22
Thurner M et al 2014 Carbon stock and density of northern boreal and temperate forests Glob. Ecol. Biogeogr. 23 297–310
Tifafi M, Guenet B and Hatté C 2018 Large differences in global and regional total soil carbon stock estimates based on soilGrids, HWSD, and NCSCD: intercomparison and evaluation based on field data from USA, England, Wales, and France Glob. Biogeochem. Cycles 32 42–56
Todd-Brown K E O et al 2014 Changes in soil organic carbon storage predicted by Earth system models during the 21st century Biogeosciences 11 2341–56
Todd-Brown K E O, Randerson J T, Post W M, Hoffman F M, Tarnocai C, Schuur E A G and Allison S D 2013 Causes of variation in soil carbon simulations from CMIP5 Earth system models and comparison with observations Biogeosciences 10 1717–36
Tokarska K B, Gillett N P, Weaver A J, Arora V K and Eby M 2016 The climate response to five trillion tonnes of carbon Nat. Clim. Change 6 851–5
Tokarska K B, Stolpe M B, Sippel S, Fischer E M, Smith C J, Lehner F and Knutti R 2020 Past warming trend constrains future warming in CMIP6 models Sci. Adv. 6 9549–67
Walters D et al 2019 The met office unified model global atmosphere 7.0/7.1 and JULES global land 7.0 configurations Geosci. Model Dev. 12 1909–63
Wan J and Crowther T W 2022 Uniting the scales of microbial biogeochemistry with trait-based modelling Funct. Ecol. 36 1457–72
Wang Y, Köhler P, He L, Doughty R, Braghiere R K, Wood J D and Frankenberg C 2021 Testing stomatal models at the stand level in deciduous angiosperm and evergreen gymnosperm forests using CliMA Land (v0.1) Geosci. Model Dev. 14 6741–63
Watanabe S et al 2011 MIROC-ESM 2010: model description and basic results of CMIP5-20c3m experiments Geosci. Model Dev. 4 845–72
Wieder W R et al 2019 Beyond static benchmarking: using experimental manipulations to evaluate land model assumptions Glob. Biogeochem. Cycles 33 1289–309
Wu T et al 2019 The Beijing climate center climate system model (BCC-CSM): the main progress from CMIP5 to CMIP6 Geosci. Model Dev. 12 1573–600
Zhang Y, Piao S, Sun Y, Rogers B M, Li X, Lian X, Liu Z, Chen A and Peñuelas J 2022 Future reversal of warming-enhanced vegetation productivity in the Northern Hemisphere Nat. Clim. Change 12 581–6
Zhao M et al 2018 The GFDL global atmosphere and land model AM4.0/LM4.0: 2. Model description, sensitivity studies, and tuning strategies J. Adv. Model. Earth Syst. 10 735–69
Zhu Z et al 2016 Greening of the Earth and its drivers Nat. Clim. Change 6 791–5